Int. J. Electrochem. Sci., 10 **(2015)** 3867 - 3884

International Journal of
ELECTROCHEMICAL
SCIENCE
www.electrochemsci.org

Graphene Oxide-Assisted Dispersion of Carbon Nanotubes in Sulfonated Chitosan-Modified Electrode for Simultaneous Detections of Sodium Nitrite, Hydroquinone, and Catechol

Yeong-Tarng Shieh[1,*], *Bo-Rung Huang*[1,2], *and Min-Lang Tsai*[2]

[1] Department of Chemical and Materials Engineering, National University of Kaohsiung, Kaohsiung 81148, Taiwan
[2] Department of Food Science, National Taiwan Ocean University, Keelung 20224, Taiwan
[*]E-mail: yts@nuk.edu.tw

Received: 27 January 2015 / *Accepted:* 5 March 2015 / *Published:* 23 March 2015

Graphene oxide (GO) and carbon nanotubes (CNT) were dispersed in chitosan (CS) or sulfonated chitosan (sCS) aqueous solution followed by casting films on glassy carbon electrodes (GCE) to investigate the electrocatalytic activities of the films by cyclic voltammetry (CV) to develop electrochemical sensors for three food additives including $NaNO_2$, hydroquinone, and catechol by cyclic voltammetry (CV). The effects of the water-soluble GO and sCS on the electrocatalytic activities of the modified electrodes and the detection abilities for the three analytes were studied. CV curves revealed that the GO/CNT/CS/GCE exhibited higher electrocatalytic activity and selective detection ability for the three analytes than the CNT/CS/GCE, GO/CS/GCE, CS/GCE, and bare GCE. The high electrocatalytic activity of the modified electrode was attributed to the well GO-assisted dispersion of the conductive CNT in the GO/CNT/CS nanocomposite film. By replacing CS with sCS, the GO/CNT/sCS/GCE exhibited more enhanced electrocatalytic activities than the GO/CNT/CS/GCE toward the oxidations of the three analytes. The enhanced electrocatalytic activities were attributed to the expandable sCS in aqueous solutions of analytes leading to enhanced porosity in the GO/CNT/sCS films. The GO/CNT/sCS 5/5/50-modified electrodes for detections of the three food additives exhibited relatively wide linear concentration ranges and relatively low limits of detections compared with those reported in literature.

Keywords: Sulfonated chitosan, graphene oxide, carbon nanotubes, chemical modified electrode, cyclic voltammetry, food additives

1. INTRODUCTION

Food additives are ingredients added to food that may help improve their texture, taste, appearance or shelf life. Sodium nitrite (or sodium nitrate) is used as a preservative, coloring and

flavoring in bacon, ham, hot dogs, luncheon meats, corned beef, smoked fish and other processed meats. This ingredient, which sounds harmless, is actually highly carcinogenic once it enters the human digestive system. Hydroquinone (HQ) has various uses that are principally associated with its action as a water-soluble reducing agent. There are various other uses associated with its reducing power. As a polymerization inhibitor, HQ prevents free radical-initiated polymerizations. In human medicine, HQ is used as a topical application in skin whitening to reduce skin color. Catechol (CC) occurs as feathery white crystals that rapidly dissolve in water and is mainly used as a precursor to pesticides, flavors, and fragrances. These phenolic compounds (HQ and CC) are commonly used as antioxidants in food in addition to many other uses.

Various methods, such as spectrophotometry [1, 2], chromatography [3], capillary electrophoresis [4, 5], chemiluminescence [6, 7], have been used to detect the above food additives. However, these analysis techniques are time-consuming. The electrochemical sensor has been considered a promising method due to its simplicity and high sensitivity. Nanoparticles have been employed as modifiers in the fabrication of chemically modified electrodes as working electrodes in electrochemical sensors. Carbon nanotubes (CNT) [8–18], for example, reportedly exhibited good electrocatalytic activities ascribed to the porous characteristic of CNT films on the surfaces of electrodes that exhibited a "thin film" effect, leading to the enhanced currents and/or lowered potentials [19–21].

Pristine CNT is hydrophobic and cannot readily disperse in water [22]. However, CNT is well dispersed in aqueous solutions of chitosan (CS), which acts as an emulsifier [23]. CS, a biocompatible polymer, is derived from the deacetylation of chitin, which is a natural polysaccharide found in a wide range of natural sources such as crustaceans, fungi, and insects. CS has various uses in areas of agriculture, medicine, food, and sewage treatment. Without modification, CS is usually insoluble in water, but is soluble in water of low pH values. Sulfonated chitosan (sCS) is water soluble due to the presence of sulfonate ($-SO_3^-$) group attached to CS. The dispersibility of CNT in CS composite film-modified electrode can affect the electrocatalytic activity of CNT in the modified electrode, with more uniform CNT dispersion giving higher electrocatalytic activity [18, 24]. To further enhance the electrocatalytic activity of CNT in CS for exploring applications in modifying the working electrode in a more sensitive biosensor device [25–27], the dispersion of CNT in CS is further improved in this study by incorporating water-soluble graphene oxides (GO), which can be obtained by oxidation of graphite using Hummer's method [28], into CS as a support for CNT to be further dispersed in CS.

The interactions between the modified working electrode and the analytes in aqueous solutions are among the factors affecting the electrocatalytic activity of the working electrode and ultimately its detection abilities for the analytes. Therefore, water-soluble sCS prepared by sulfonations of CS is also investigated to replace CS to enhance interactions between the working electrode and the three analytes in aqueous solutions (i.e., $NaNO_2$, HQ, and CC). The effects of GO and sCS on the electrocatalytic activities of the modified electrodes and the detection abilities for the three analytes are investigated. This study showed that the never-reported GO/CNT/sCS-modified working electrode exhibits simultaneous detection abilities and high detection sensitivities for the three analytes. The modified electrodes using GO and sCS can enhance the biosensor performance much higher than the electrodes without using them.

2. EXPERIMENTAL

2.1 Materials

GO was prepared by oxidation of graphite powders. In a typical experiment, 1 g of graphite powder (300 mesh in particle size, 99% in purity, supplied by Alfa Aesar) was added in 70 mL of HNO_3 and 0.5 g of $NaNO_3$ under stirring at 4 °C, at which 6 g of $KMnO_4$ was added. The solution was continuously stirred for 10 min and then stirred at 35 °C for 6 h. Deionized (DI) water (46 mL) was gradually added in 15 min followed by additions of 140 mL of DI water and 20 mL of H_2O_2 (30%) under ultrasonic vibrations for 1 h. The reaction mixture was filtered using a membrane with 0.2 μm pore size. The product on the membrane was rinsed with 40 mL of HCl (5%) aqueous solution, collected, and dissolved in 2000 mL of DI water. The supernatant of the solution was filtered using a membrane with 0.2 μm pore size. The product on the membrane was dried at 60 °C for 24 h and was determined to be GO by Fourier transform infrared spectrometer (FTIR, Perkin-Elmer Spectrum Two).

CNT was synthesized by thermal chemical vapor deposition at 750 °C for 1 h. Acetylene was used as a carbon source, and ferrocene was used as a catalyst in a quartz tube furnace in our laboratories [22]. The deposited product was examined by transmission electron microscopy (TEM, JEOL JEM-100CXII at 300 kV), and consisted of multi-walled CNT. The synthesized CNT was approximately 20–30 nm in diameter and about 1 μm in length.

CS, which was supplied by the Charming & Beauty Corporation (Taiwan), had average molecular weight of 350,000 g/mol and degree of deacetylation of approximately 97%. sCS was prepared according to literature [29, 30]. In a typical experiment, 1 g of CS was added to a mixture of 40 mL of H_2SO_4 (98%) and 20 mL of $HClSO_3$ (98%), which had been previously cooled at 0–4 °C. The solution was then heated to 25 °C under stirring for 30 min. The solution was poured into 750 mL of cold diethyl ether to precipitate the product. The precipitate was collected by filtering, dissolved in 150 mL of water, neutralized with 2 N NaOH, dialyzed against water for 3 d, and dried for 24 h.

2.2 Preparations of GO/CNT/sCS solutions and GO/CNT/sCS-modified GCE

5 mg of GO powder and/or 5 mg of CNT powder were added in 5 mL of aqueous solution containing 5 or 50 mg of dissolved sCS to obtain solutions of GO/sCS 5/5, CNT/sCS 5/5, GO/CNT/sCS 5/5/5, and GO/CNT/sCS 5/5/50 under ultrasonication for 10 min. 10 μL of each solution was cast on a prepolished glassy carbon electrode (GCE) and allowed to dry in ambient air to obtain GO/sCS 5/5- CNT/sCS 5/5-, GO/CNT/sCS 5/5/5-, and GO/CNT/sCS 5/5/50-modified GCE. For comparison purposes, GO/CS 5/5- CNT/CS 5/5-, GO/CNT/CS 5/5/5-, and GO/CNT/CS 5/5/50-modified GCE were also prepared similar to the above procedures except that 5 mL of aqueous solution containing 2% acetic acid was used to dissolve CS.

For characterizations of surface morphologies, 10 μL of each solution prepared as above was cast on an indium tin oxide (ITO) glass plate and allowed to dry in ambient air. A field emission scanning electron microscopy (FESEM, HITACHI S-4800) was used for characterizations of surface morphologies at an operating voltage of 1 KeV.

2.3 Electrochemical measurements

A potentiostat (CH611D, CH Instruments) was used to perform CV analyses at 25 °C in a conventional three-electrode system with GCE as the working electrode, a platinum wire as auxiliary electrode, and Ag/AgCl/3M KCl as reference electrode. The phosphate buffer solution (PBS) of pH 7.4 containing 0.1 M KCl was used as the background electrolyte in experiments. The modified GCE was immersed in the PBS containing $NaNO_2$, HQ, and CC (all supplied by Sigma-Aldrich) to conduct CV between −0.4 and 1.0 V at a scan rate of 50 mV/s. The GCE has a round active area with 3 mm diameter. The second CV cycle was used for all investigations. Each prepared modified GCE should pass stability test by immersion in 2 mM solution of the $Fe(CN)_6^{3-/4-}$ redox couple used as a probe and by scanning for 30 CV cycles with at least 90% remaining in current intensity. For reproducibility tests, two modified GCEs were prepared by each composite. The peak currents of the second CV scans for the two modified GCEs were also compared. Only peak currents that were negligibly different were adopted in this paper.

2.4 Amperometric analyses of the GO/CNT/sCS 5/5/50-modified GCE

Amperometric analyses were conducted by successive additions (2, 2, 4, 4, 8, 8, 12, 16, 20, 40, 60, 80, 100, 120, 140, 160, 180, and 200 μL) of 5 mM of each $NaNO_2$, HQ, and CC aqueous solution at every 50 s in 8 mL of 0.1 M phosphate buffer (pH 7.4) aqueous solution at an operating potential of 0.75, 0.1, and 0.2 V, respectively. The plots of the responding anodic currents vs. time can produce the plots of currents vs. concentrations for $NaNO_2$, HQ, and CC. From these plots, the linear range of concentrations, the limit of detection, the sensitivity of detection, and the response time can be determined.

3. RESULTS AND DISCUSSION

3.1 Characterizations of GO/CNT/CS and GO/CNT/sCS nanocomposite films

Figure 1a shows the FTIR spectra of GO and reduced graphene oxide (rGO). As seen in Figure 1a, bands for GO at 1060, 1625, 1740, and 3400 cm^{-1} correspond to stretching vibrations of C-O, C=C, C=O, and O-H, respectively. This finding indicates that oxidations of graphite have occurred to form characteristic C-O, C=O, and O-H groups on GO, leading to water solubility. Upon reduction, these bands for GO disappear (Figure 1a), and water insoluble rGO is obtained. Figure 1b shows the FTIR spectra before and after sulfonation reactions of CS. Following sulfonation reactions, the intensity of the overlapped peaks for NH_2 and H-bonded OH groups in CS near 3300 cm^{-1} decreases and that of free OH groups in sCS near 3500 cm^{-1} appears, an indication that the reactions have resulted in consumptions of NH_2 and OH groups in CS. Two newly appeared peaks for sCS near 800 and 1230 cm^{-1}, which characterize the stretching vibration of C-O-S and asymmetric stretching vibration of SO_2,

indicate the formations of -SO_3H and/or -SO_3Na groups in sCS. Given the presence of the sulfonate groups in sCS, sCS is water soluble, whereas CS can dissolve only in acidic aqueous solutions.

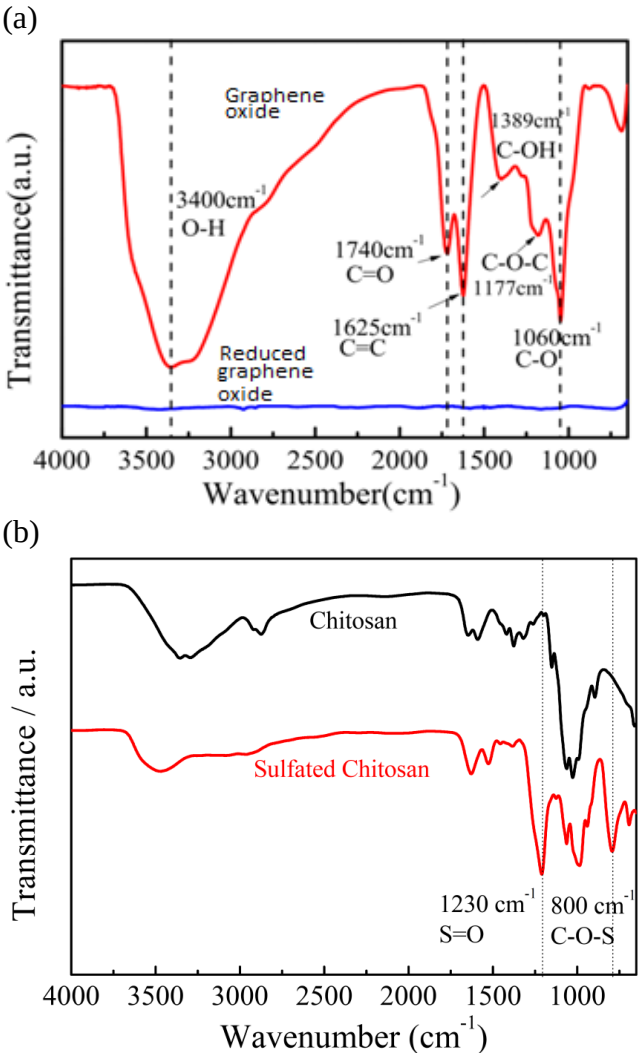

Figure 1. FTIR spectra of (a) graphene oxide (GO) and reduced graphene oxide (rGO), (b) chitosan (CS), and sulfonated chitosan (sCS).

Considering that the dispersibilities of the nanoparticles (GO and CNT) in the CS or sCS composite films would affect the electrocatalytic activities of the composites to redox reactions of the analytes, FESEM images of the composites were investigated. As seen in Figure 2, wrinkled foil-like GO (Figure 2b) is dispersed on CS, which appears to be a uniform film (Figure 2a). Entangled CNT is seen without much CS on CNT (Figure 2c). In the presence of GO, some CS is seen to adhere to CNT in the composite of GO/CNT/CS 5/5/5 (Figure 3a), which appears to be a perforate film. With more amount of CS added (Figure 3b), a film without any hole can be obtained. Some CNTs are uncovered and are exposed on the surface of the film, although most GO and CNT are embedded in CS (Figure 3b). By replacing CS with sCS, GO and CNT are glued by sCS in GO/CNT/sCS 5/5/5, giving a nonwoven mat-like film as in Figure 3c. With an increase in amount of sCS (Figure 3d), the nonwoven

mat-like film appears to be denser in surface morphology with segregated sCS on surface. How the surface morphologies of the films affect the electrocatalytic activities of the modified electrodes and thus their detection abilities for the three food additives ($NaNO_2$, HQ, and CC) is investigated and presented in the following sections.

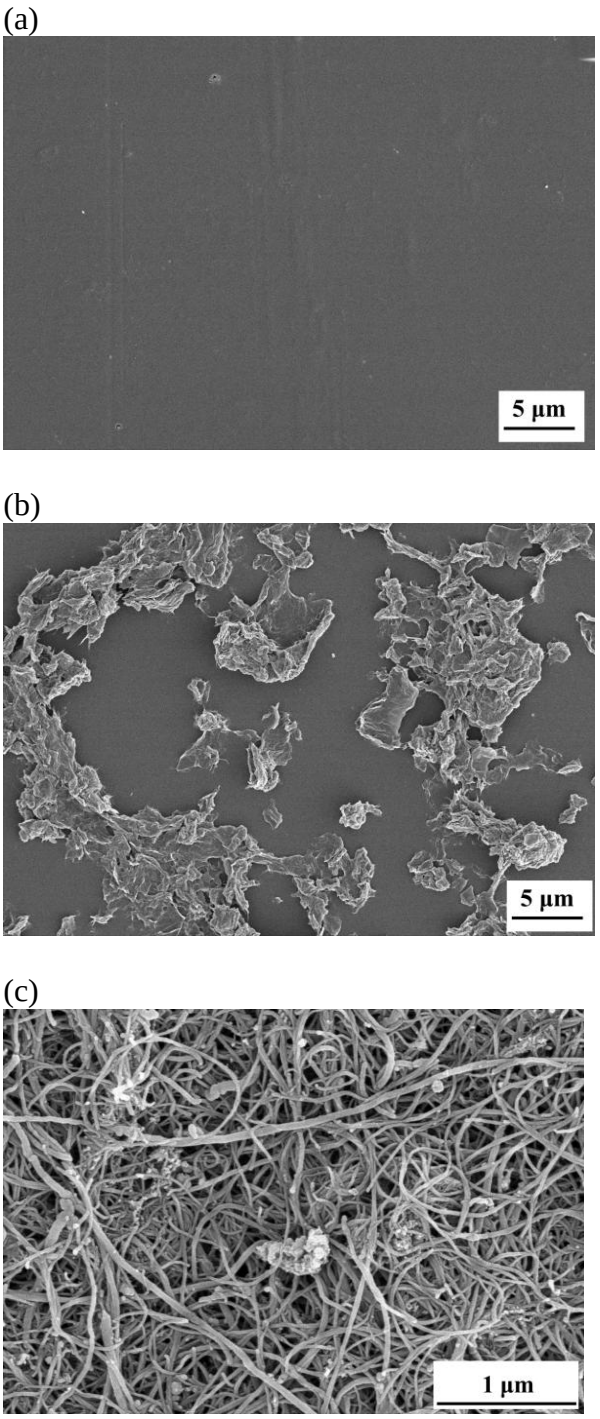

Figure 2. FESEM images of the (a) CS, (b) GO/CS, and (c) CNT/CS. GO, CNT, and CS were all 5 mg each in the film.

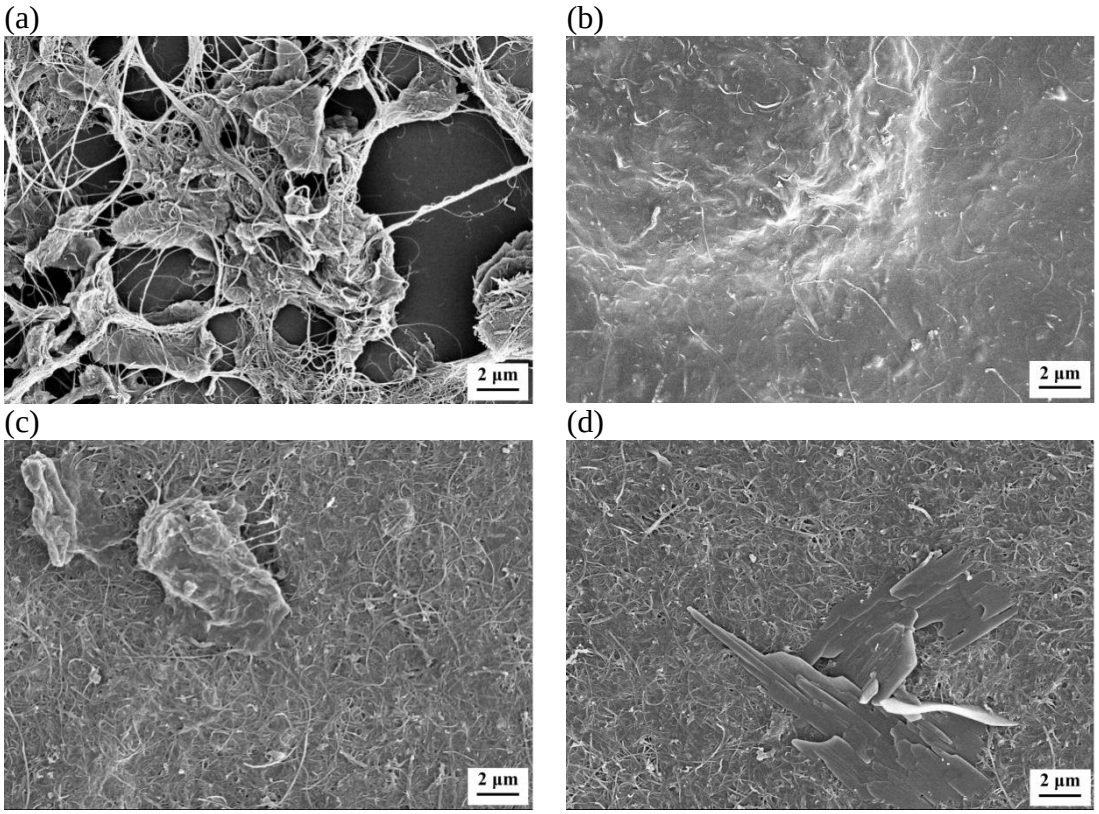

Figure 3. FESEM images of (a) GO/CNT/CS 5/5/5, (b) GO/CNT/CS 5/5/50, (c) GO/CNT/sCS 5/5/5, and (d) GO/CNT/sCS 5/5/50.

3.2 Detection ability of the GO/CNT/CS- and GO/CNT/sCS-modified GCE for $NaNO_2$, HQ, and CC

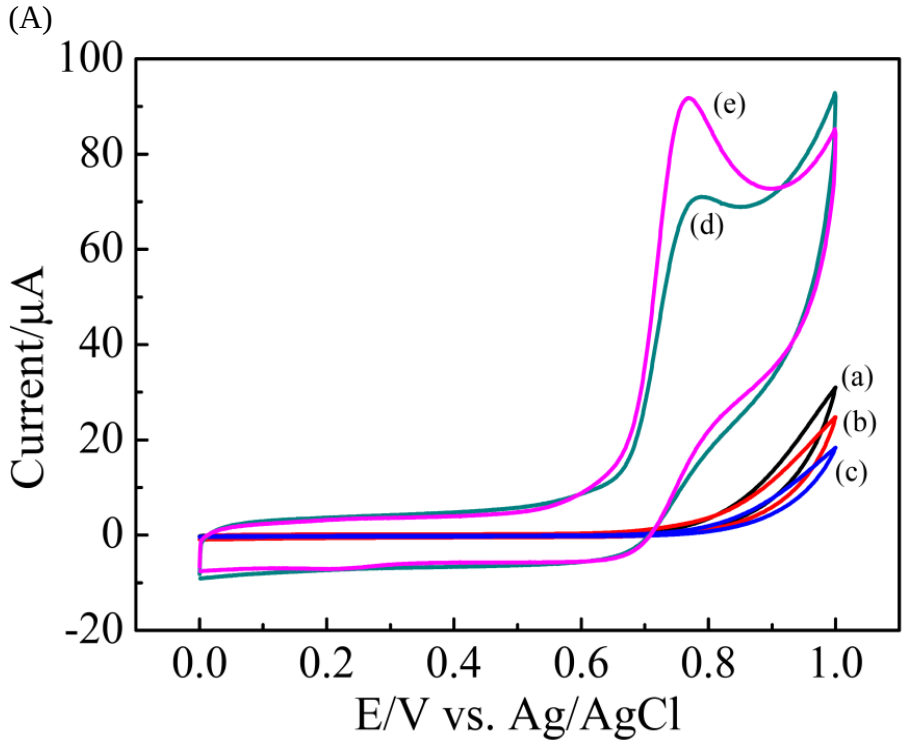

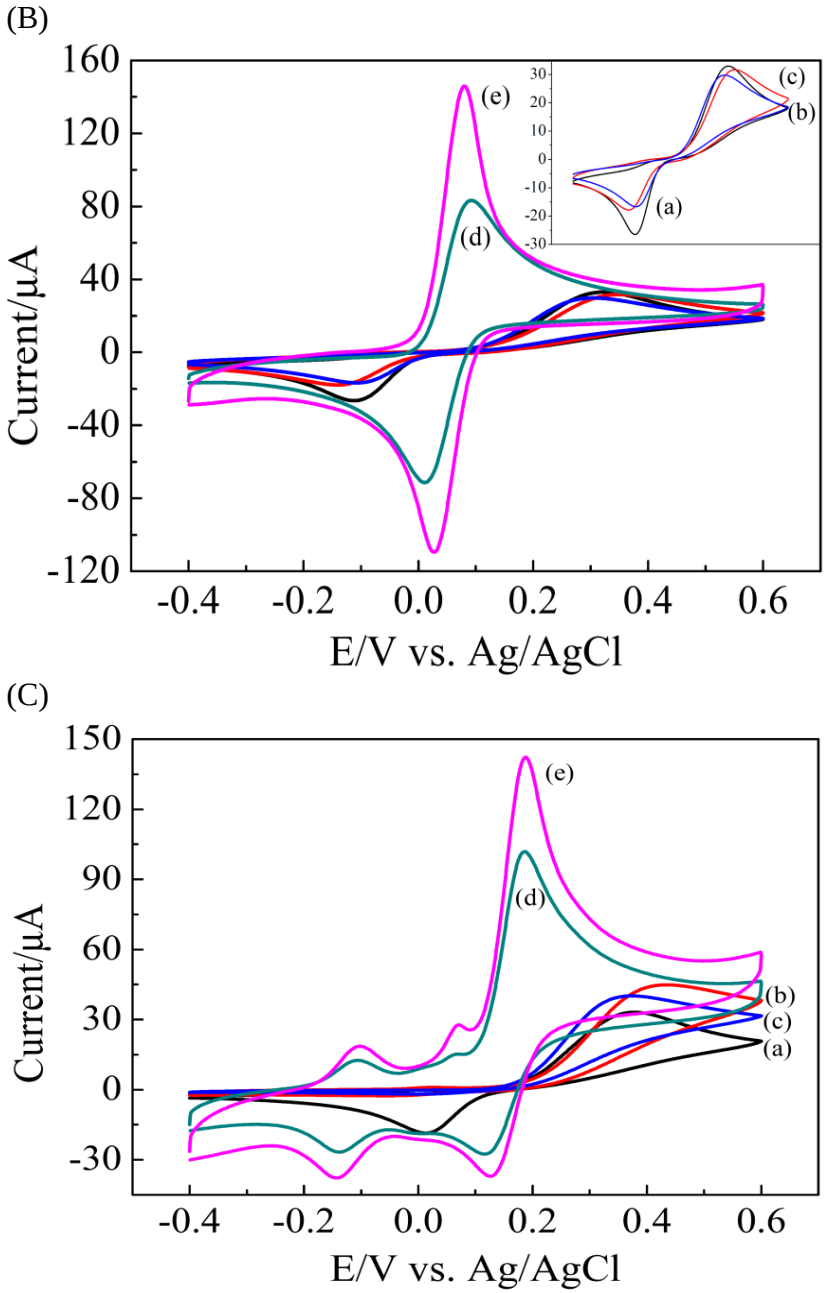

Figure 4. CV curves recorded at (a) bare GCE, (b) CS/GCE, (c) GO/CS/GCE, (d) CNT/CS/GCE, and (e) GO/CNT/CS/GCE for (A) 2 mM $NaNO_2$, (B) 2 mM HQ, and (C) 2 mM CC in 0.1 M pH 7.4 PBS containing 0.1 M KCl. GO, CNT, and CS were all 5 mg each. Scan rate: 50 mV s^{-1}.

Figure 4 compares the CV curves recorded at bare GCE, pure CS-modified GCE, and CS composite-modified GCE for the three food additives, namely, $NaNO_2$, HQ, and CC. Bare GCE, CS/GCE, and GO/CS/GCE are found to give insignificant current responses to all three analytes. The additions of CNT in CNT/CS/GCE and GO/CNT/CS/GCE result in significantly enhanced current responses, as seen in curves d and e in Figure 4. Although GO is low in conductivity, its presence in GO/CNT/CS/GCE further enhances the anodic peak currents for all three analytes compared with CNT/CS/GCE. CNT/CS/GCE exhibits enhanced anodic peak current compared with bare GCE and CS/GCE. This finding can be attributed to improved dispersion of CNT by the presence of GO. Studies

[31–34] showed that GO could act as a support for CNT to reside at and thus lead to improved dispersion of CNT and further enhanced anodic current response. The $NaNO_2$ has an anodic peak near 0.75 V but has no cathodic peak due to its irreversible oxidation reaction. HQ exhibits anodic and cathodic peaks near 0.1 and 0.02 V, respectively, corresponding to the reversible oxidation and reduction reactions of HQ. CC exhibits two anodic peaks near −0.1 and 0.19 V and two cathodic peaks near −0.15 and 0.11 V, corresponding to two reversible oxidation and reduction reactions of CC.

Compared with the bare GCE, the significantly increased peak currents for GO/CNT/CS/GCE (Figure 4) indicate that the GO/CNT/CS-modified GCE exhibits electrocatalytic activities to oxidation reactions of all three analytes. The anodic peak current gives an insignificant change with an increase in the amount of CS (curves b and c in Figure 5).

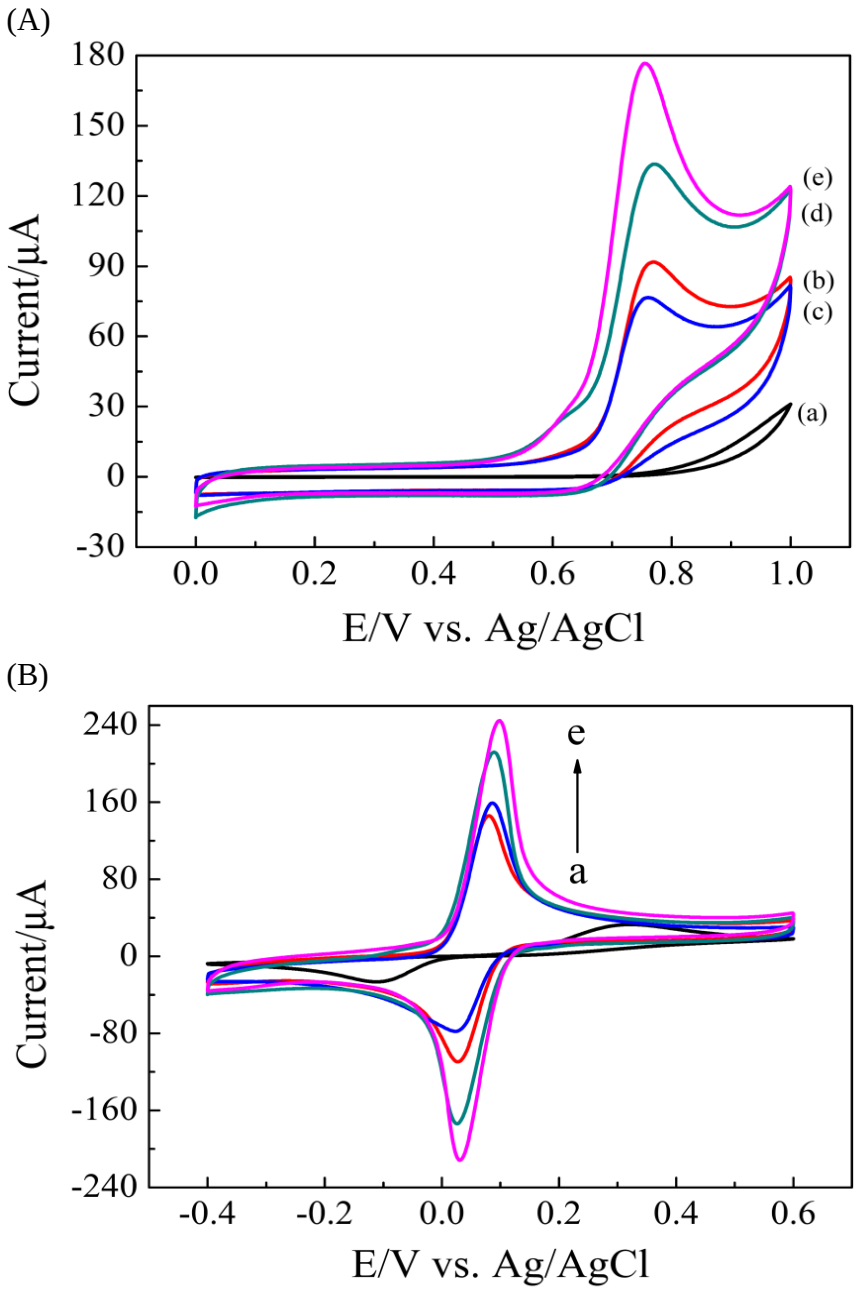

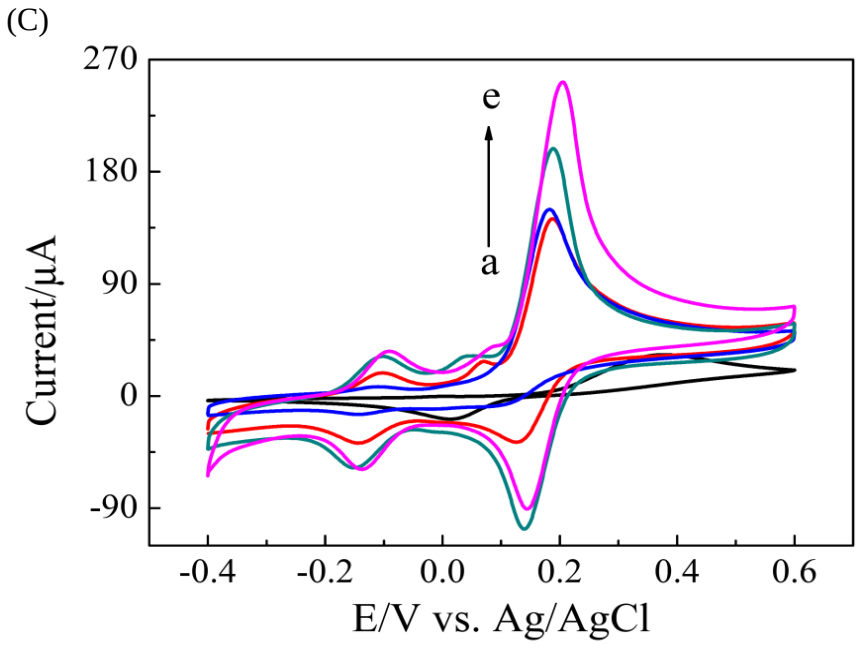

Figure 5. CV curves recorded at (a) bare GCE, (b) GO/CNT/CS 5/5/5-, (c) GO/CNT/CS 5/5/50-, (d) GO/CNT/sCS 5/5/5-, and (e) GO/CNT/sCS 5/5/50-modified GCE for (A) 2 mM $NaNO_2$, (B) 2 mM HQ, and (C) 2 mM CC in 0.1 M pH 7.4 PBS containing 0.1 M KCl. Scan rate: 50 mV s^{-1}.

However, following a replacement of CS by sCS, the GO/CNT/sCS-modified GCE exhibits a clear increase in the anodic peak current, which increases with increasing amount of sCS used (curves d and e in Figure 5). For the GO/CNT/sCS/GCE, swollen composite film on GCE was visually observed after CV scans due to the water-soluble sCS as a result of the presence of -SO_3H and/or -SO_3Na groups in sCS. This phenomenon may be responsible for the further increase in the anodic peak current (curve d in Figure 5) compared with CS as a matrix (curve b in Figure 5). The swelling of sCS allows increases in porosity in the GO/CNT/sCS films and results in a "thin film" effect [19–21], leading to increases in the anodic peak currents. The anodic peak currents increase further (curve e in Figure 5) for all three analytes with increase of sCS in GO/CNT/sCS 5/5/50.

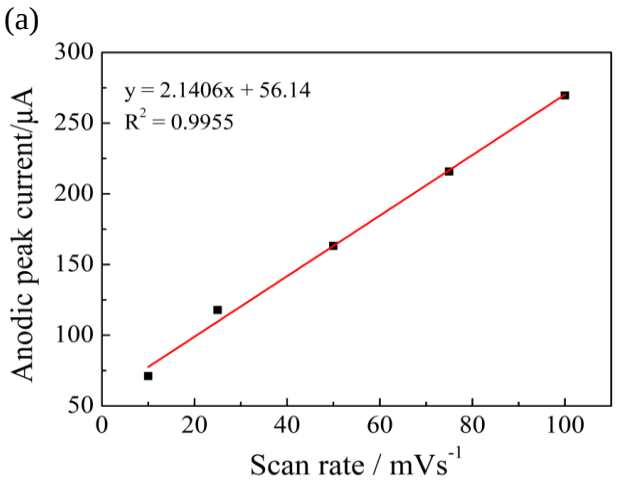

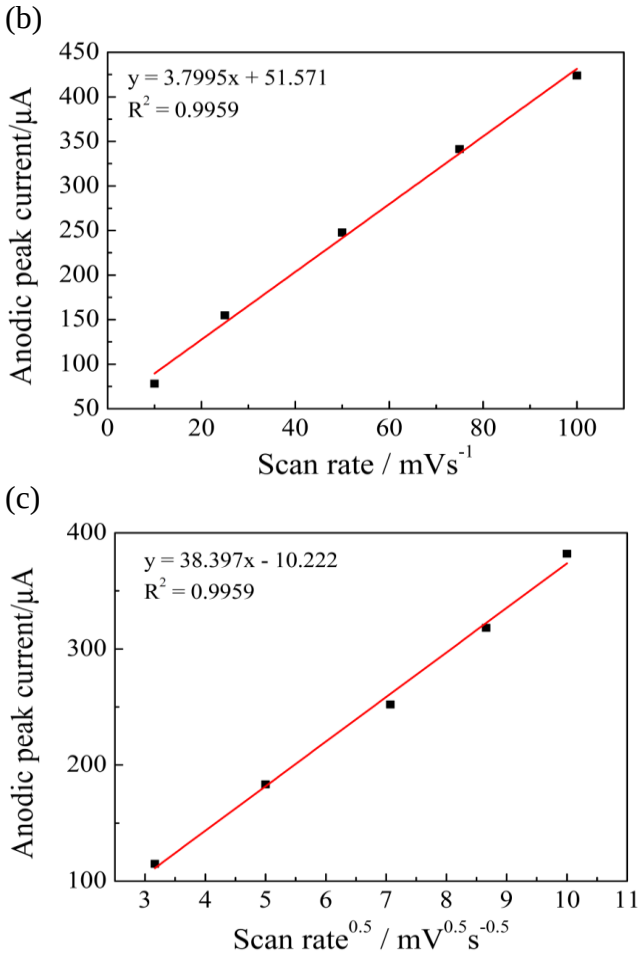

Figure 6. Plots of anodic peak currents recorded at GO/CNT/sCS 5/5/50-modified GCE in 2 mM of (a) $NaNO_2$, (b) HQ, and (c) CC in 0.1 M pH 7.4 PBS containing 0.1 M KCl as a function of scan rates (or scan rates$^{1/2}$) of 10, 25, 50, 75, and 100 mV s^{-1}.

Figure 6 shows the anodic peak currents for the three analytes as plotted vs. scan rate or scan rate$^{1/2}$. Figure 6 shows that the anodic peak currents are linearly increasing with increasing scan rates for $NaNO_2$ and HQ but with increasing scan rate$^{1/2}$ for CC, as recorded at GO/CNT/sCS 5/5/50-modified GCE.

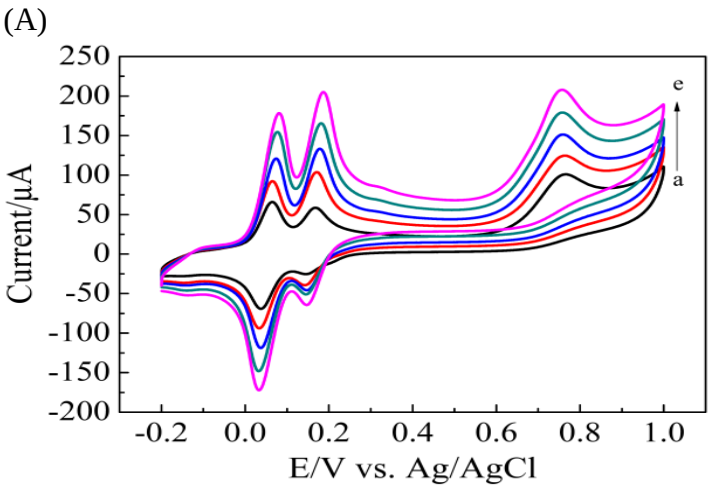

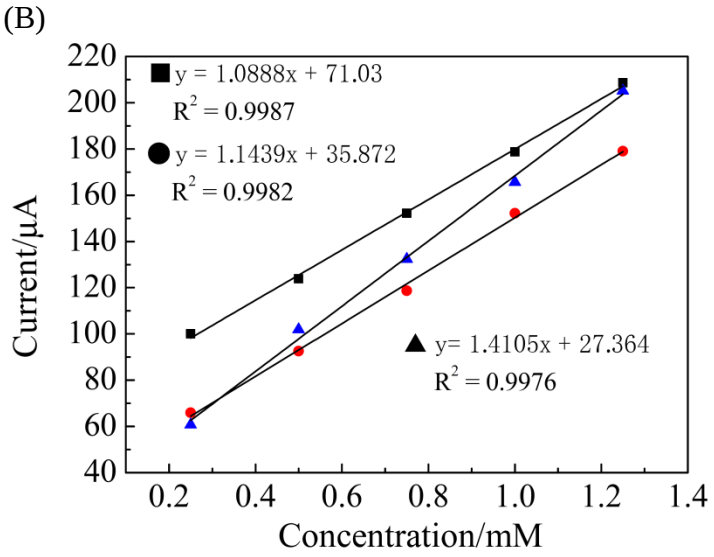

Figure 7. (A) CV responses of the GO/CNT/sCS 5/5/50-modified GCE upon the simultaneous increases of concentrations of $NaNO_2$, HQ, and CC, all being at 0.25, 0.5, 0.75, 1, and 1.25 mM (curves a–e) in 0.1 M pH 7.4 PBS containing 0.1 M KCl at a scan rate of 50 mV s^{-1}. (B) Anodic peak currents in (A) as plotted versus concentrations of (■) $NaNO_2$, (●) HQ, and (▲) CC.

This finding indicates that the GO/CNT/sCS/GCE follows surface adsorption-controlled kinetics for oxidation of $NaNO_2$ and HQ but diffusion-controlled kinetics for oxidations of CC [35]. Figure 6 thereby suggests that the interactions of the analytes with the GO/CNT/sCS/GCE fall in the order of CC > HQ > $NaNO_2$. This high-to-low order is seen to be consistent with the sensitivities of detections for the three analytes in Figure 7, with an increase in the interaction of an analyte with the modified electrode giving an increase in sensitivity of its detection. The strong electrocatalytic activity of the GO/CNT/sCS 5/5/50-modified GCE gave rise to strong anodic peak currents for all three analytes, which exhibit separated anodic peaks at different voltages in their respective CV curves (curves e in Figure 5). This activity allows simultaneous detections of the three analytes (Figure 7A). The corresponding three anodic peaks are well resolved in the same CV curve. Figure 7A indicates that the three analytes can be detected not only simultaneously but also selectively and quantitatively in a linear range of concentrations from 0.25 mM to 1.25 mM (Figure 7B). The sensitivity of detection for CC is the highest followed by that for HQ and for $NaNO_2$ (Figure 7B). The results in Figure 7B are consistent with those found in terms of surface interactions in Figure 6.

3.3 Amperometric analyses of the GO/CNT/sCS-modified GCE for $NaNO_2$, HQ, and CC

The method of amperometric current (i)–time (t) response was used to determine the response in current as a function of concentrations of $NaNO_2$, HQ, and CC for the GO/CNT/sCS 5/5/50-modified GCE, which was chosen for the amperometric analyses because of its high electrocatalytic activity to the oxidation reactions of the three food additives.

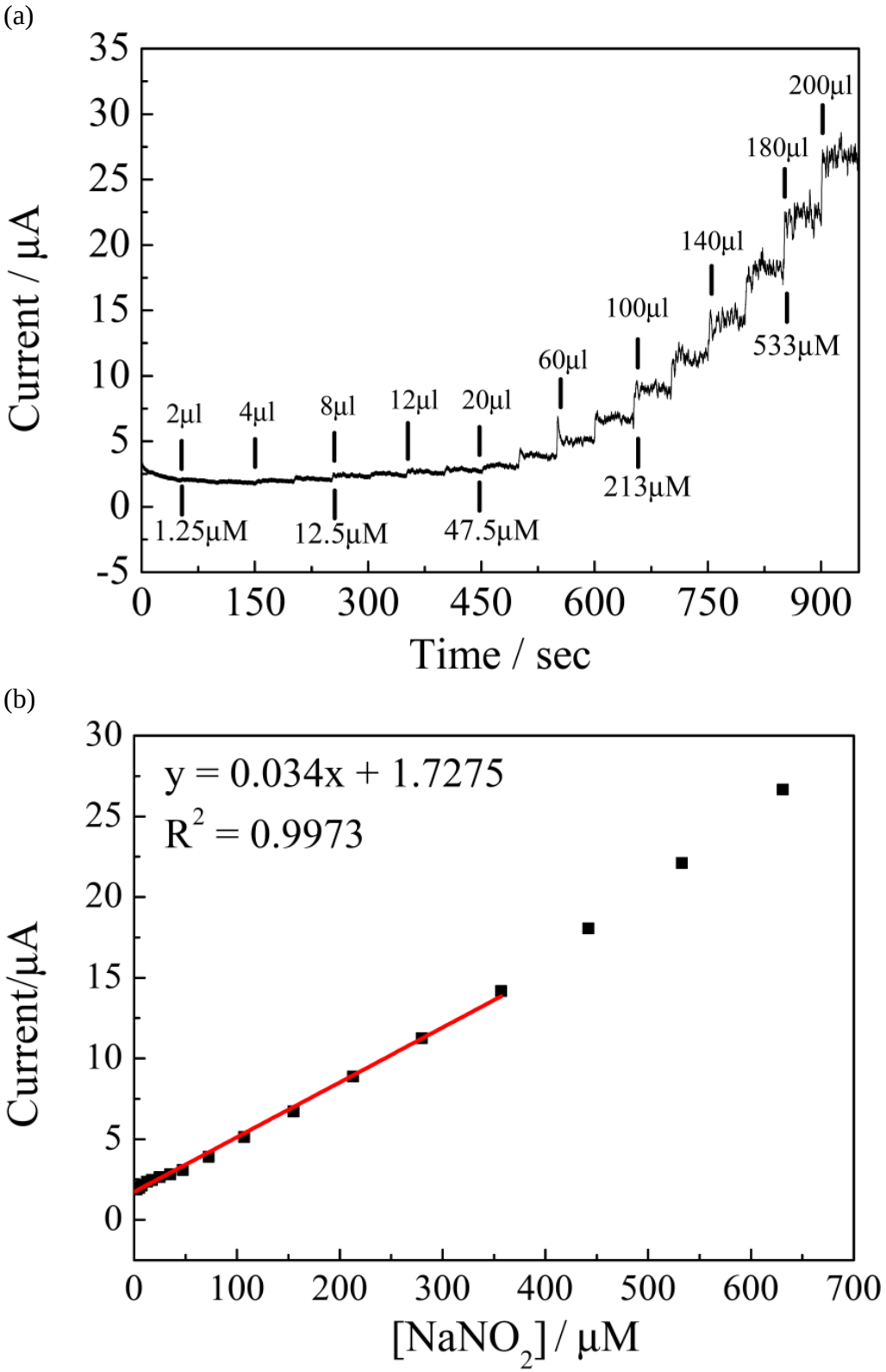

Figure 8. (a) Amperometric responses of the GO/CNT/sCS 5/5/50-modified GCE upon successive additions every 50 s of 2, 2, 4, 4, 8, 8, 12, 16, 20, 40, 60, 80, 100, 120, 140, 160, 180, and 200 μL each of 5 mM $NaNO_2$ in 0.1 M PBS (pH 7.4, containing 0.1 M KCl) at an operating potential of +0.75 V. (b) Linear regression analysis of the $NaNO_2$ concentration–current curves.

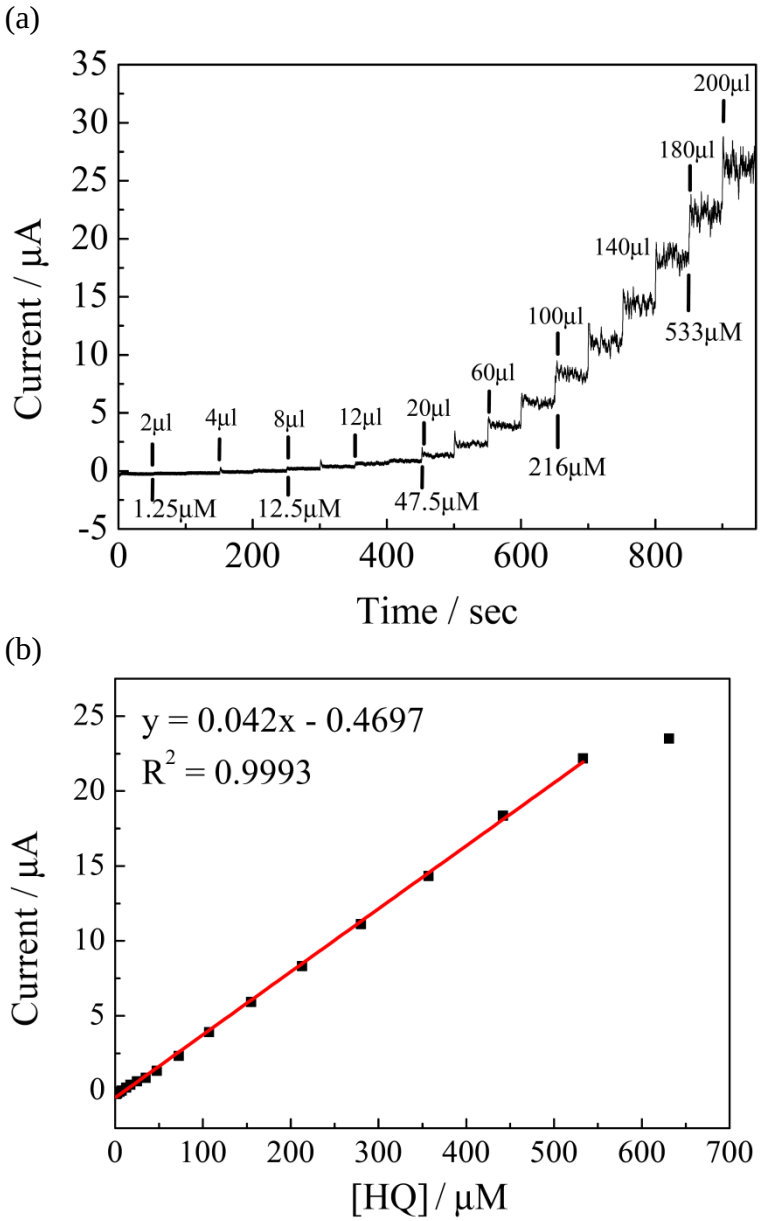

Figure 9 (a) Amperometric responses of the GO/CNT/sCS 5/5/50-modified GCE upon successive additions every 50 s of 2, 2, 4, 4, 8, 8, 12, 16, 20, 40, 60, 80, 100, 120, 140, 160, 180, and 200 µL each of 5 mM HQ in 0.1 M PBS (pH 7.4, containing 0.1 M KCl) at an operating potential of +0.1 V. (b) Linear regression analysis of the HQ concentration–current curves.

The response time of the sensor, which can be obtained by the i–t plots, was defined as the time for the sensor's response to reach from 10% to 90% of its final value after analyte addition. The linear range of concentration, the limit of detection, and the sensitivity of detection can be obtained from the plots of the responded current vs. concentrations of the three analytes. Figures 8a, 9a, and 10a show the amperometric response of the GO/CNT/sCS 5/5/50-modified GCE upon successive additions every 50 s of a small volume of 5 mM of $NaNO_2$, HQ, and CC, at operating potentials of 0.75, 0.1, and 0.2 V, respectively.

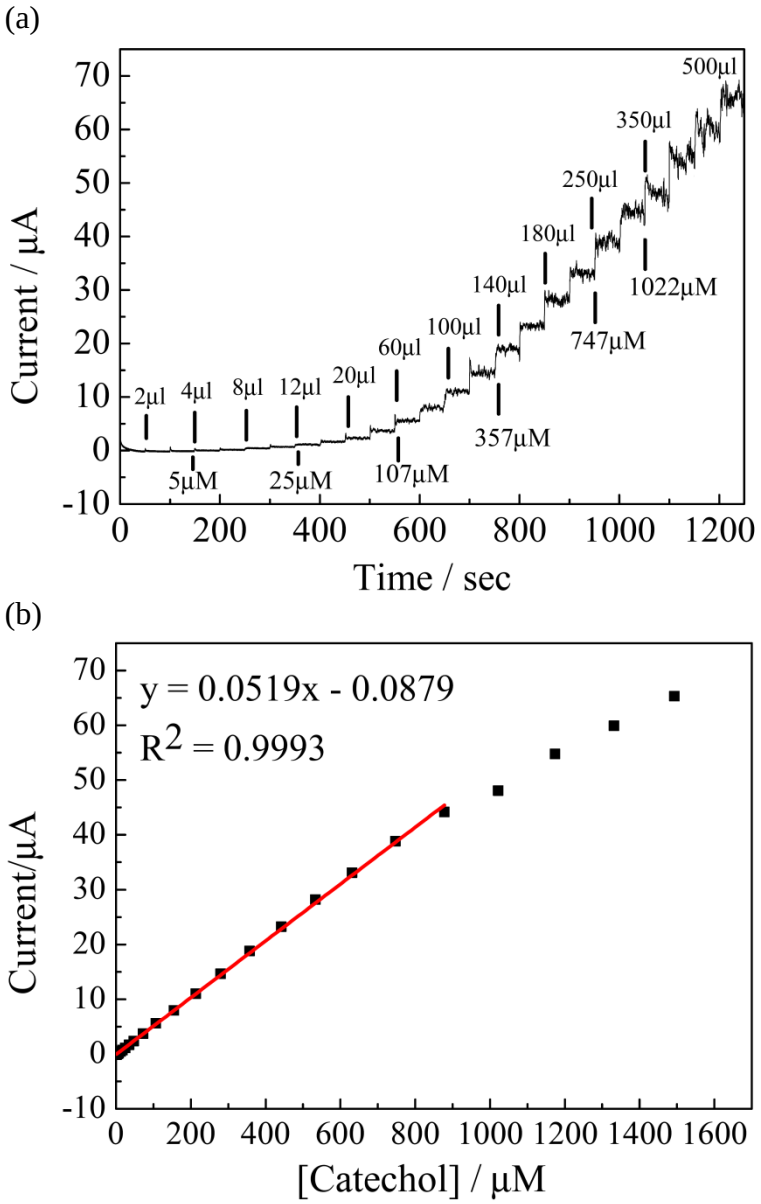

Figure 10. (a) Amperometric responses of the GO/CNT/sCS 5/5/50-modified GCE upon successive additions every 50 s of 2, 2, 4, 4, 8, 8, 12, 16, 20, 40, 60, 80, 100, 120, 140, 160, 180, and 200 µL each of 5 mM CC in 0.1 M PBS (pH 7.4, containing 0.1 M KCl) at an operating potential of +0.2 V. (b) Linear regression analysis of the CC concentration–current curves.

Figures 8b, 9b, and 10b show the calibration curves of currents vs. concentrations for the three analytes. As seen in Figures 8b, 9b, and 10b, the rates of increasing currents with concentrations of $NaNO_2$, HQ, and CC, namely, the sensitivities of detections, were 0.481, 0.594, and 0.734 µA cm^{-2} μM^{-1}, respectively, for the GO/CNT/sCS 5/5/50-modified GCE. These values were obtained from the slopes in the plots of currents vs. concentrations by considering the circled active area with a diameter of 3 mm on the GCE. The sensitivities of detections fell in the order of CC > HQ > $NaNO_2$, which is consistent with the high-to-low order in Figure 7, in which the three analytes can be selectively detected. Response times of 0.9, 0.7, and 0.6 s were obtained after each addition of $NaNO_2$, HQ, and

CC, respectively. The linear ranges of concentrations for $NaNO_2$, HQ, and CC were 1.25–357, 1.25–533, and 1.25–878 μM, respectively. The linear ranges of concentrations of the sensor were defined as the regressed linear range with R^2 more than 0.995 in the plots of the responded currents vs. concentrations. The limits of detections (LOD) with signal-to-noise (S/N) ratio of 3.3 for $NaNO_2$, HQ, and CC were 0.048, 0.022, and 0.020 μM, respectively. The LOD (S/N = 3.3) was determined by the following equation: LOD = 3.3 × (standard deviation of *y* intercept)/(slope of the fitted line in the plot of current (*y*) vs. concentration (*x*)). The sensitivities of detections, linear ranges of concentrations, LOD (S/N = 3.3), and response times for $NaNO_2$, HQ, and CC recorded at the GO/CNT/sCS 5/5/50-modified electrode are tabulated in Table 1. In comparison with the modified electrodes reported in literature [36–38], the GO/CNT/sCS 5/5/50-modified electrodes for detection of the three food additives in this study exhibited relatively wide linear concentration ranges and relatively low LOD.

Table 1. Detection sensitivity, linear range, limit of detection, and response time for sodium nitrite, hydroquinone, and catechol as recorded at the GO/CNT/sCS 5/5/50-modified electrode.

Food additives	Sensitivity ($\mu A\ cm^{-2}\ \mu M^{-1}$)	Linear range (μM)	Limit of detection (μM)	Response time (s)
$NaNO_2$	0.481	1.25–357	0.048	0.9
Hydroquinone	0.594	1.25–533	0.022	0.7
Catechol	0.734	1.25–878	0.020	0.6

4. CONCLUSIONS

Nanocomposite films of GO and CNT in CS or sCS that were cast on GCE were found to have high electrocatalytic activities toward oxidations of three food additives ($NaNO_2$, HQ, and CC) and exhibited simultaneous detection abilities for the three analytes. The high electrocatalytic activities of the modified electrodes were attributed to the well GO-assisted dispersion of the conductive CNT in the GO/CNT/CS nanocomposite films. By replacing CS with sCS, the GO/CNT/sCS/GCE exhibited more enhanced electrocatalytic activities than the GO/CNT/CS/GCE toward the oxidations of the three analytes. The enhanced electrocatalytic activities were attributed to the expandable sCS in aqueous solutions of analytes, leading to enhanced porosity in the GO/CNT/sCS films. At the GO/CNT/sCS 5/5/50-modified GCE, the linear concentration ranges for $NaNO_2$, HQ, and CC detections were 1.25–357, 1.25–533, and 1.25–878 μM, respectively. Sensitivities of detections were 0.481 ($NaNO_2$), 0.594 (HQ), and 0.734 (CC) $\mu A\ cm^{-2}\ \mu M^{-1}$. The LOD were 0.048 ($NaNO_2$), 0.022 (HQ), and 0.020 μM (CC).

ACKNOWLEDGEMENT
We thank the National Science Council of Taiwan for their financial support for this study under contract NSC 102-2221-E-390-025

References

1. V. V. Kuznetsov, S. V. Zemyatova, *J. Anal. Chem.,* 62 (2007) 637
2. W. J. Dong, J. P. Song, C. Dong, M. M. F. Choi, *Chinese Chemical Letters,* 21 (2010) 346
3. P. Niedzielski, I. Kurzyca, J. Siepak, *Anal. Chim. Acta,* 577 (2006) 220
4. J. H. Wang, W. H. Huang, Y. M. Liu, J. K. Cheng, J. Yang, *Anal Chem.,* 76 (2004) 5393
5. Y. R. Wang, H. W. Chen, *Journal of Chromatography A,* 1080 (2005) 191
6. A. Lagalante, P. Greenbacker, *Anal. Chim. Acta,* 590 (2007) 151
7. A. Ogawa, H. Arai, H. Tanizawa, T. Miyahara, T. Toyo'oka, *Analytica Chimica Acta,* 383 (1999) 221
8. B. J. Sanghavi, A. K. Srivastava, *Electrochim. Acta,* 55 (2010) 8638
9. D. Salinas-Torres, F. Huerta, F. Montilla, E. Morallon, *Electrochim. Acta,* 56 (2011) 2464
10. W. Guo, L. Xu, F. Li, B. Xu, Y. Yang, S. Liu, Z. Sun, *Electrochim. Acta,* 55 (2010) 1523
11. B. Ge, Y. Tan, Q. Xie, M. Ma, S. Yao, *Sens. Actuators B,* 137 (2009) 547
12. G. Li, J. Hao, *J. Electrochem. Soc.,* 156 (2009) K134
13. H. L. Pang, J. Liu, D. Hu, X. H. Zhang, J. H. Chen, *Electrochim. Acta,* 55 (2010) 6611
14. Y. T. Shieh, T. Y. Yu, T. L. Wang, C. H. Yang, *J. Electroanal. Chem.,* 664 (2012) 139
15. Y. T. Shieh, T. Y. Yu, T. L. Wang, C. H. Yang, W. T. Liao, *Colloid Polym. Sci.,* 290 (2012) 1
16. Y. T. Shieh, Y. A. Chen, R. H. Lin, T. L. Wang, C. H. Yang, *Electrochim. Acta,* 76 (2012) 518
17. Y. T. Shieh, J. J. Jung, R. H. Lin, C. H. Yang, T. L. Wang, *J. Electrochem. Soc.,* 159 (2012) H921
18. Y. T. Shieh, Y. Y. Tu, T. L. Wang, R. H. Lin, C. H. Yang, Y. K. Twu, *Journal of Electroanalytical Chemistry,* 704 (2013) 190
19. M. C. Henstridge, E. J.F. Dickinson, M. Aslanoglu, C. Batchelor-McAuley, R. G. Compton, *Sens. Actuators B,* 145 (2010) 417
20. B R. Kozub, N. V. Rees, R. G. Compton, *Sens. Actuators B,* 143 (2010) 539
21. I. Streeter, G. G. Wildgoose, L. Shao, R. G. Compton, *Sens. Actuators B,* 133 (2008) 462
22. Y. T. Shieh, G. L. Liu, H. H. Wu, C. C. Lee, *Carbon,* 45 (2007) 1880
23. Y. T. Shieh, H. M. Wu, Y. K. Twu, Y. C. Chung, *Colloid and Polymer Science,* 288 (2010) 377
24. Y. T. Shieh, Y. C. Tsai, Y. K. Twu, *Int. J. Electrochemical Science,* 8 (2013) 831
25. J. Li, Q. Liu, Y. J. Liu, S. C. Liu, S. Z. Yao, *Anal. Biochem.,* 346 (2005)107
26. S. Bollo, N. F. Ferreyra, G. A. Rivas, *Electroanalysis,* 19 (2007) 833
27. P. Gomathi, M. K. Kim, J. J. Park, D. Ragupathy, A. Rajendran, S. C. Lee, J. C. Kim, S. H. Lee, H. D. Ghim, *Sens. Actuators B,* 155 (2011) 897
28. W. S. Hummers Jr., R. E. Offeman, *J. Am. Chem. Soc.,* 80 (1958) 1339
29. Q. Tian, X. H. Wang, W. Wang, C. N. Zhang, P. Wang, Z. Yuan, *Nanomedicine: Nanotechnology, Biology, and Medicine,* 8 (2012) 870
30. M. Terbojevich, C. Carraro, A. Cosani, *Makromol Chem,* 190 (1989) 2847
31. L. Tian, M. J. Meziani, F. Lu, C. Y. Kong, L. Cao, T. J. Thorne, and Y. P. Sun, *ACS Applied Materials and Interfaces,* 2 (2010) 3217
32. H. Wang, S. Li, Y. Si, N. Zhang, Z. Sun, H. Wu, and Y. Lin, *Nanoscale,* 6 (2014) 8107-8116.
33. C. Zhang, L. Ren, X. Wang, and T. Liu, *J Phys Chem C,* 114 (2010) 11435
34. L. Qiu, X. Yang, X. Gou, W. Yang, Z.F. Ma, G. G. Wallace, and D. Li, *Chemisstry-A European Journal,* 16 (2010) 10653
35. A. J. Bard, L. R. Faulkner, *Electrochemical methods, fundamentals and applications,* John Wiley and Sons Inc., New York (1980)

36. J. Hong, Z. Dai, *Sensors and Actuators B: Chemical*, 140 (2009) 222
37. D. Yuan, S. Chen, F. Hu, C. Wang, R. Yuan, *Sensors and Actuators B: Chemical*, 168 (2012) 193
38. Y. Y. Tan, X. X. Guo, J. H. Zhang, J. Q. Kan, *Biosensors and Bioelectronics*, 25 (2010) 1681